Chiral Electrodynamics and Cosmic Magnetic Fields

1. Basics on Magnetic Field Evolution
2. A general approach to the chiral magnetic effect
3. The chiral effect in hot neutron stars and in the early Universe
4. Conclusions and outlook

DFG Deutsche Forschungsgemeinschaft

PROJEKTTRÄGER FÜR DAS Bundesministerium für Bildung und Forschung

UHH Universität Hamburg
DER FORSCHUNG | DER LEHRE | DER BILDUNG

Günter Sigl
II. Institut theoretische Physik, Universität Hamburg

The Magnetic Universe:
Understanding the origin and evolution of B fields

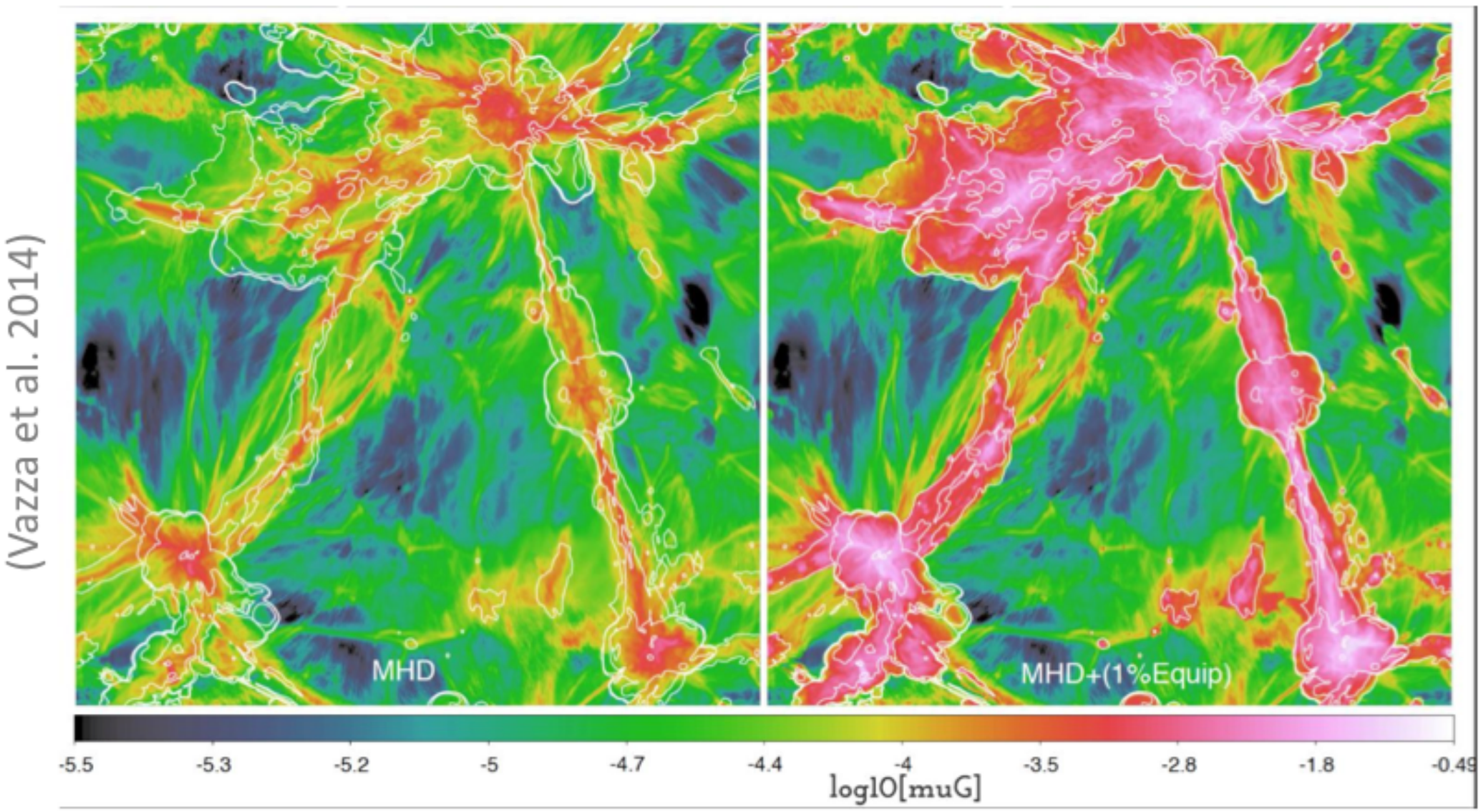

- Determine the role of magnetism in regulating galaxy evolution
- Detection and characterization of the magnetic cosmic web
- Magnetic evolution of AGN over cosmic time

Observations and simulations of the non-thermal Universe

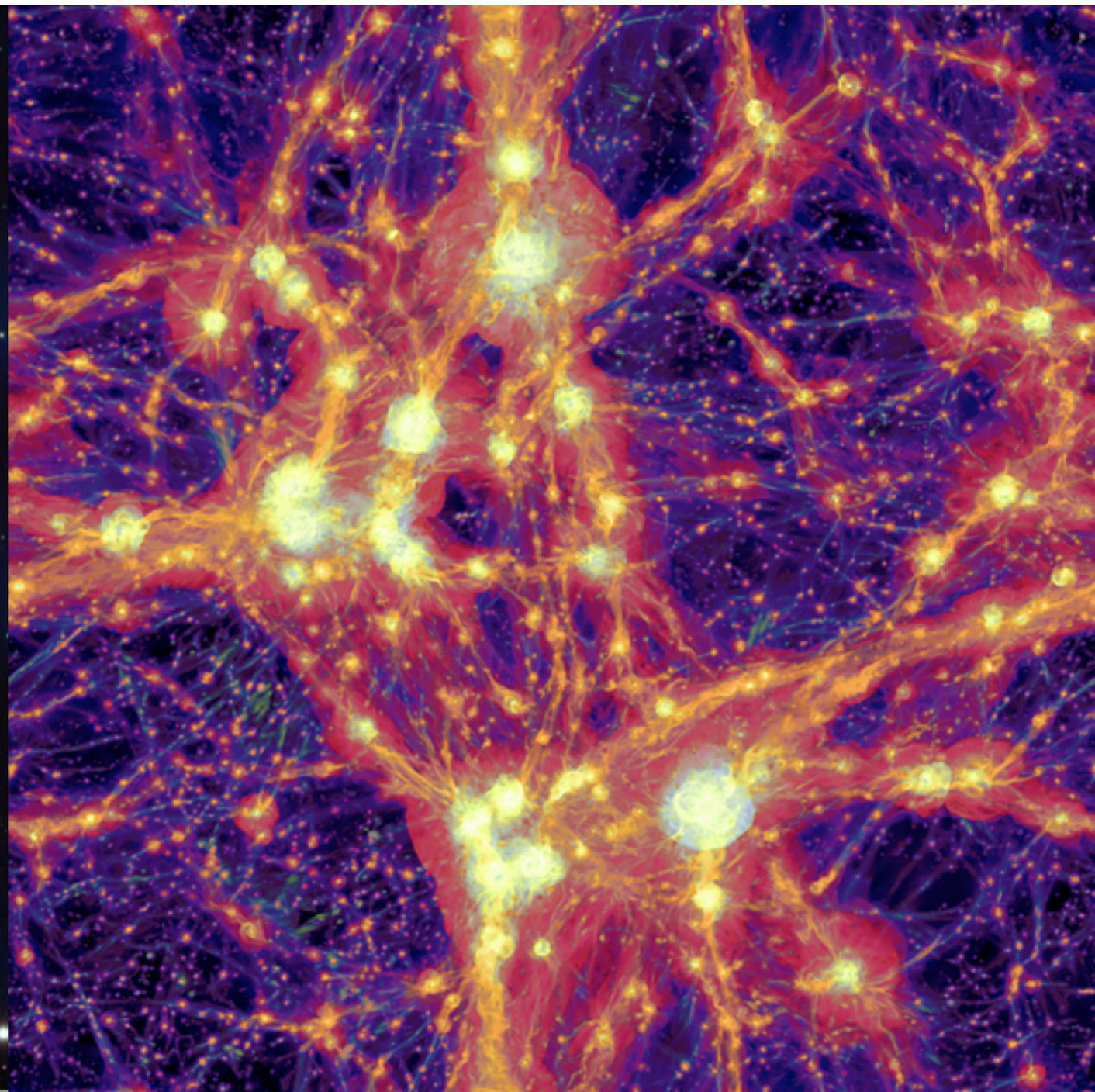

Structured Extragalactic Magnetic Fields

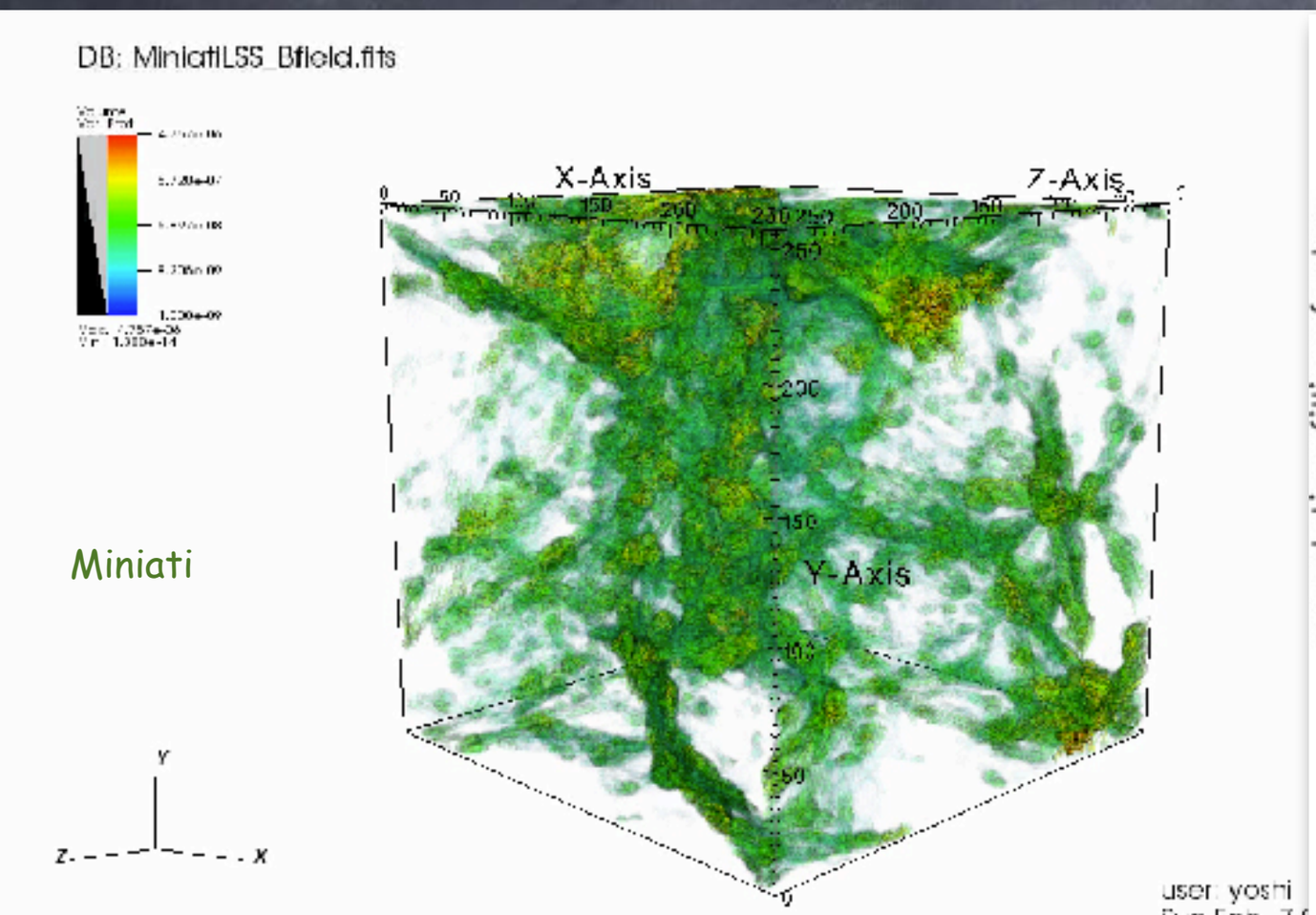

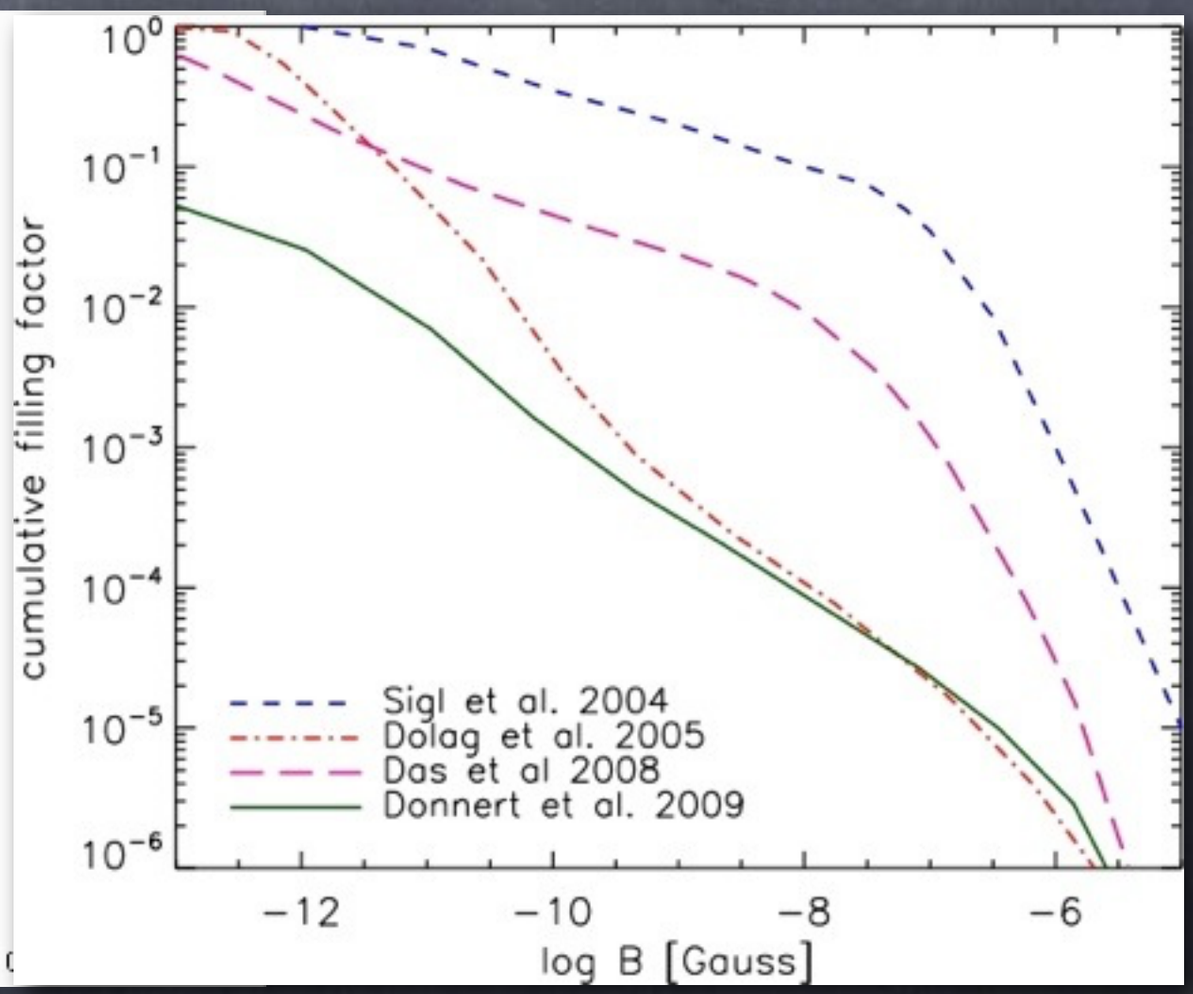

Kotera, Olinto, Ann.Rev.Astron.Astrophys. 49 (2011) 119

Filling factors of extragalactic magnetic fields are not well known, depend on initial conditions and come out different in different large scale structure simulations

EGMF - Origin

The origin of EGMF is still uncertain - mainly two different seed mechanisms:

- Astrophysical scenario: Seed magnetic fields are generated during structure formation (e.g. by a Biermann Battery [Biermann, 1950]) and are then amplified by the dynamo effect [Zeldovich et al., 1980]
- Cosmological scenario: Strong seed magnetic fields are generated in the Early Universe, e.g. at a phase transition (QCD, electroweak) [Sigl et al., 1997] or during inflation [Turner and Widrow, 1988], and some of the initial energy content is transfered to larger scales.

The latter are the so-called primordial magnetic fields and will be focused on in the following.

- Basics for the time evolution: Homogeneous and isotropic magnetohydrodynamics in an expanding Universe.

Primordial Magnetic fields - Simple Estimates

The main problem is that the comoving horizon at the temperature T_g of creation is very small,

$$l_{H,0} \sim \frac{T_g}{T_0}\frac{1}{H(T_g)} \simeq 0.2\left(\frac{100\,\mathrm{MeV}}{T_g}\right)\,\mathrm{pc}\,,$$

so that length scales of interest today are far in the tail.
A magnetic field in equipartition with radiation corresponds to $B \simeq 3\times 10^{-6}\,\mathrm{G}$.

On the other hand, if there is rough equipartition between kinetic and magnetic turbulence, $v_{rms} \sim v_A = B/(4\pi)^{1/2}$, and coherence length is comparable to size of eddy which turns once in a Hubble time, one gets a relation between field amplitude B_0 and coherence length $l_{c,0}$,

$$l_c \sim \frac{v_{\rm A}}{H}\,, \quad B_0(T) \propto T l_{c,0}(T)\,,$$

$$l_{c,0} \sim 1 \left(\frac{B_0}{10^{-14}\,{\rm G}}\right)\,{\rm pc}\,.$$

if magnetic fields are close to maximally helical, i.e. $\langle \boldsymbol{A}\,\boldsymbol{B}\rangle \sim +\!- \, l_c B^2$, helicity conservation yields $l_{c,0}(T)B_0(T)^2 \sim$ const.

Summary of Current Constraints

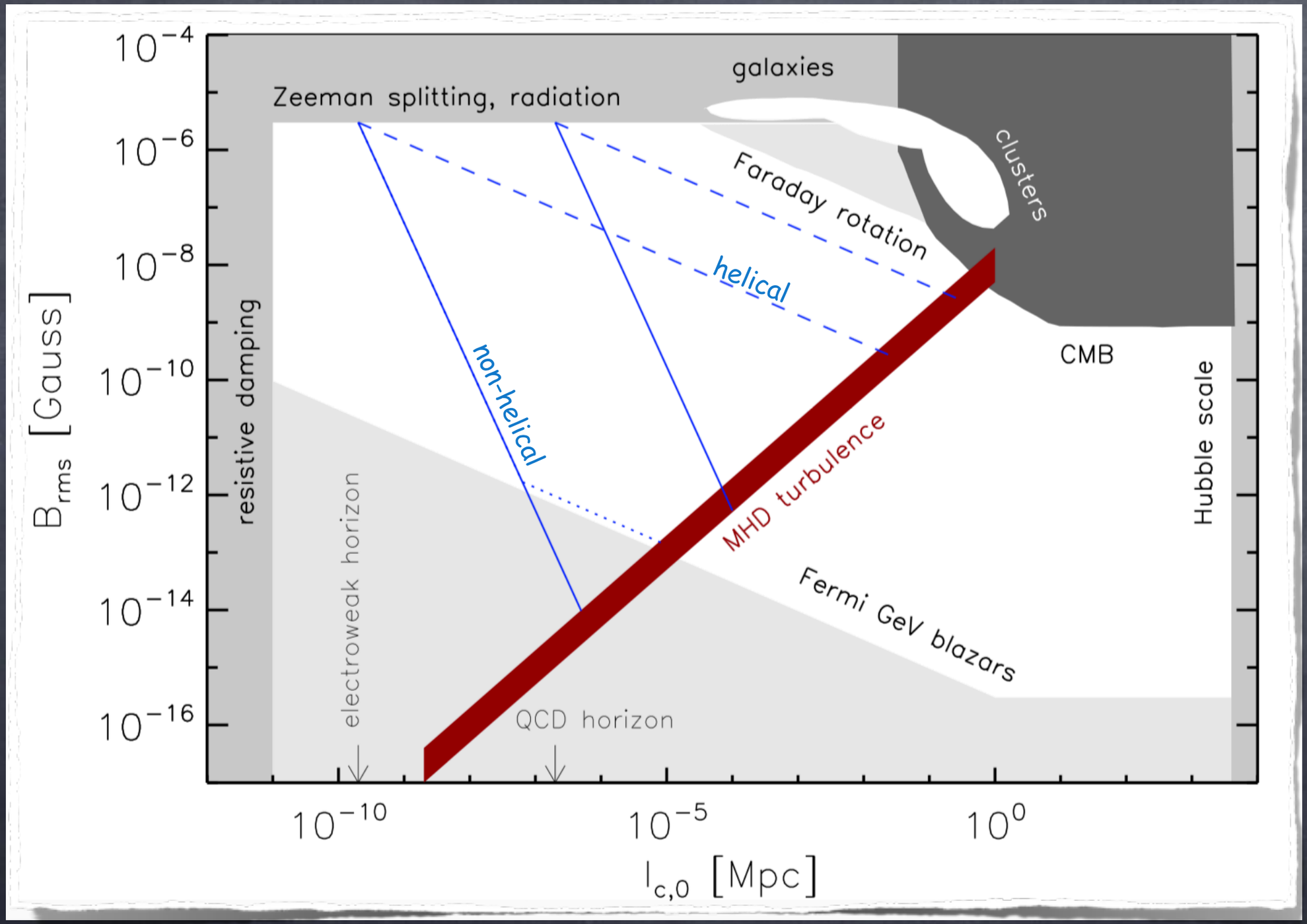

G. Sigl, book "Astroparticle Physics: Theory and Phenomenology", Atlantis Press 2016

partly based on A. Neronov, I. Vovk, Science 328, 73 (2010)

Primordial Magnetic fields - Basic MHD

Magnetohydrodynamics (MHD)

- Maxwell's equations:
  $\nabla \cdot \mathbf{B} = 0,\ \nabla \times \mathbf{E} = -\partial_t \mathbf{B},\ \nabla \times \mathbf{B} = 4\pi \mathbf{j}$
- Continuity equation for mass density ρ: $\partial_t \rho + \nabla(\rho \mathbf{v}) = 0$
- Navier-Stokes equations:

$$\rho\left(\partial_t \mathbf{v} + (\mathbf{v}\nabla)\,\mathbf{v}\right) = -\nabla p + \mu \Delta \mathbf{v} + (\lambda + \mu)\nabla\left(\nabla \mathbf{v}\right) + \mathbf{f}$$

For the magnetic field and the turbulent fluid it follows therefore

$$\partial_t \mathbf{B} = \frac{1}{4\pi\sigma}\Delta \mathbf{B} + \nabla \times (\mathbf{v} \times \mathbf{B})$$

$$\partial_t \mathbf{v} = -\left(\mathbf{v}\nabla\right)\mathbf{v} + \frac{(\nabla \times \mathbf{B}) \times \mathbf{B}}{4\pi\rho} + \mathbf{f}_v.$$

Primordial Magnetic fields - Basic MHD

- Switch to Fourier (k-)space: $B(\mathbf{x}) \rightarrow \hat{B}(\mathbf{q})$, $v(\mathbf{x}) \rightarrow \hat{v}(\mathbf{q})$

$$\partial_t \hat{\mathbf{B}}(\mathbf{q}) = -\frac{1}{4\pi\sigma} q^2 \hat{\mathbf{B}}(\mathbf{q}) + \frac{iV^{\frac{1}{2}}}{(2\pi)^{\frac{3}{2}}} \mathbf{q} \times \left[\int \mathrm{d}^3 k \left(\hat{\mathbf{v}}(\mathbf{q}-\mathbf{k}) \times \hat{\mathbf{B}}(\mathbf{k}) \right) \right]$$

$$\partial_t \hat{\mathbf{v}}(\mathbf{q}) = -\frac{iV^{\frac{1}{2}}}{(2\pi)^{\frac{3}{2}}} \int \mathrm{d}^3 k \left[(\hat{\mathbf{v}}(\mathbf{q}-\mathbf{k}) \cdot \mathbf{k}) \, \hat{\mathbf{v}}(\mathbf{k}) \right]$$

$$+ \frac{iV^{\frac{1}{2}}}{(2\pi)^{\frac{3}{2}}} \frac{1}{4\pi\rho} \int d^3 k \left[\left(\mathbf{k} \times \hat{\mathbf{B}}(\mathbf{k}) \right) \times \hat{\mathbf{B}}(\mathbf{q}-\mathbf{k}) \right]. \tag{1}$$

Terms of the type $\hat{\mathbf{v}}(\mathbf{q}-\mathbf{k}) \times \hat{\mathbf{B}}(\mathbf{k})$ describe mode-mode coupling such that power from small length scales $1/k$ can be transported to large length scales $1/q$.

based on Saveliev, Jedamzik, Sigl, PRD 86, 103010 (2012), PRD 87, 123001 (2013)

Primordial Magnetic Fields - Correlation Function

Aim: Computation of the correlation function for B and v

- Homogeneity: The correlation function cannot depend on the position in space
- Isotropy: The correlation function only depends on the magnitude of the spatial separation

In Fourier space this means that the most general Ansatz is [de Kármán and Howarth, 1938]

$$\langle \hat{B}(\mathbf{k})\hat{B}(\mathbf{k}')\rangle \sim \delta(\mathbf{k}-\mathbf{k}')[(\delta_{lm}-\frac{k_l k_m}{k^2})\frac{M_k}{k^2}+i\epsilon_{lmj}\frac{k_j}{k}H_k^m]$$

$$\langle \hat{v}(\mathbf{k})\hat{v}(\mathbf{k}')\rangle \sim \delta(\mathbf{k}-\mathbf{k}')[(\delta_{lm}-\frac{k_l k_m}{k^2})\frac{U_k}{k^2}+i\epsilon_{lmj}\frac{k_j}{k}H_k^v]$$

Master Equations for the Power Spectra

In the absence of helicity, $H_k^m = H_k^v = 0$, the master equation for the magnetic field power spectrum then reads

$$\begin{aligned}\langle \partial_t M_q \rangle = \int_0^\infty \mathrm{d}k \Bigg\{ \Delta t \int_0^\pi \mathrm{d}\theta \Bigg[& -\frac{1}{2}\frac{q^2 k^4}{k_1^4} \sin^3\theta \langle M_q \rangle \langle U_{k_1} \rangle + \\ & + \frac{1}{2}\frac{q^4}{k_1^4}\left(q^2 + k^2 - qk\cos\theta\right)\sin^3\theta \langle M_k \rangle \langle U_{k_1} \rangle \\ & - \frac{1}{4}q^2\left(3 - \cos^2\theta\right)\sin\theta \langle M_k \rangle \langle M_q \rangle \Bigg] \Bigg\},\end{aligned}$$

where θ is the angle between $\mathbf{q}$ and $\mathbf{k}$.

Primordial Magnetic Fields: Full-Blown Numerical MHD Simulations versus semi-analytical methods based on transport equations

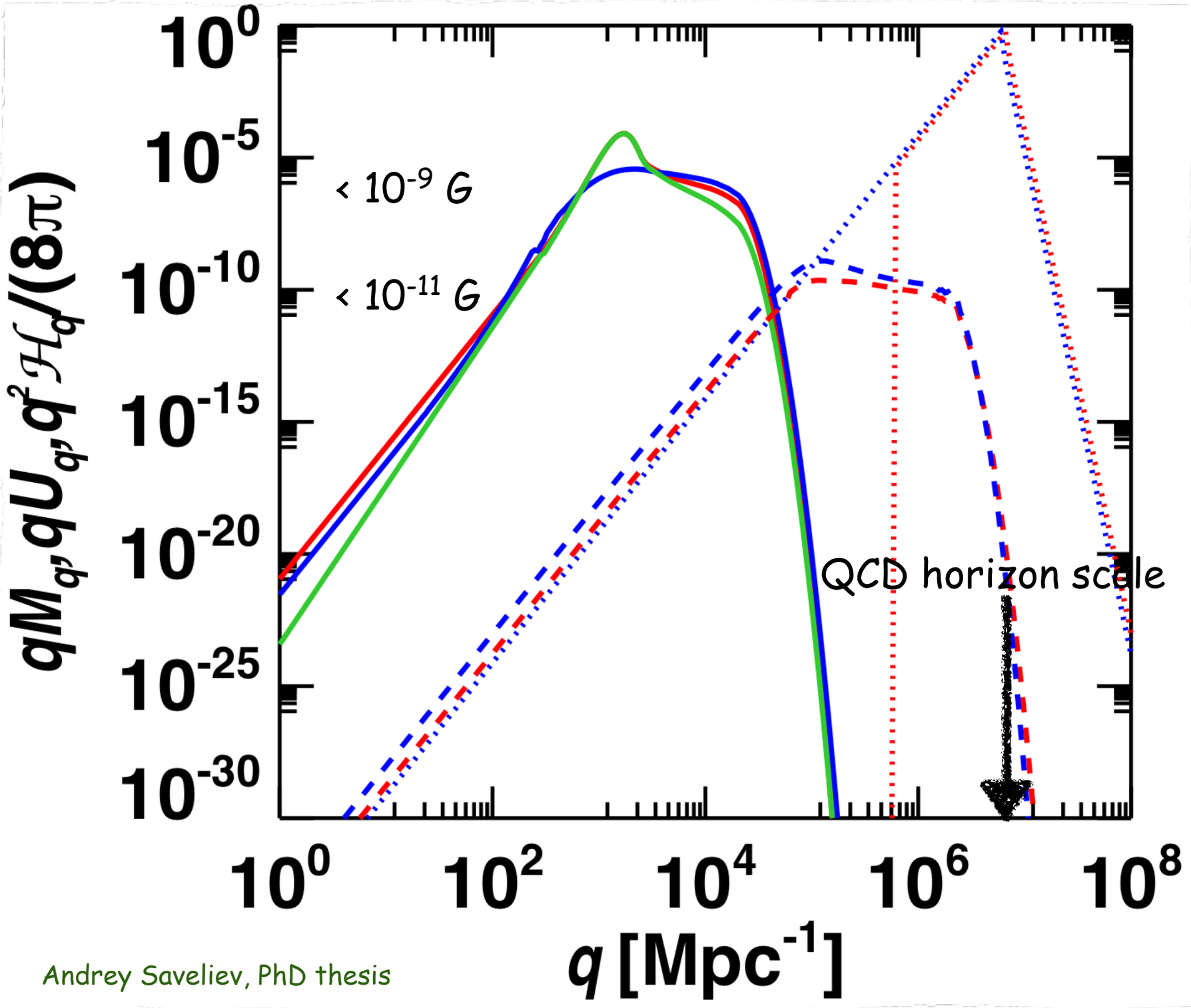

Andrey Saveliev, PhD thesis

normalized to turbulence energy, < 10^{-6} G

magnetic fields

turbulent velocity

magnetic helicity

dotted = initial condition

dashed = final state without helicity

solid = final state with maximal helicity

A General Approach to the Chiral Magnetic Effect as a Possible Source of Magnetic Helicity

Some literature:

M. E. Shaposhnikov, Nucl.Phys. B299 797-817 (1988)

A. Vilenkin, Phys. Rev. D 22, 3080 (1980)

N. Yamamoto, Phys.Rev. D93, 065017 (2016)

Boyarsky, J. Fröhlich, and O. Ruchayskiy, Phys. Rev. Lett. 108, 031301 (2012)

A. Boyarsky, J. Fröhlich, O. Ruchayskiy, Phys. Rev. D 92, 043004 (2015)

H. Tashiro, T. Vachaspati, A. Vilenkin, PRD 86, 105033 (2012)

L. Campanelli, Phys.Rev.Lett. 98 251302 (2007)

papers by Dvornikov and Semikoz, in particular Phys. Rev. D 95, 043538 (2016)

papers by Leite, Pavlovic and Sigl

We here use Gaussian natural units, $\varepsilon_0 = 1/(4\pi)$ and $\mu_0 = 4\pi$, respectively.

Note that also often used in the literature are Lorentz-Heaviside units for which $\varepsilon_0 = \mu_0 = 1$.

The current of left-chiral minus right-chiral charges satisfies

$$\partial_\mu \left(j^\mu_L - j^\mu_R \right) = \frac{e^2}{8\pi^2} F_{\mu\nu} \tilde{F}^{\mu\nu} = -\frac{e^2}{2\pi^2} \mathbf{E} \cdot \mathbf{B} \, .$$

In thermal equilibrium a magnetic field leads to a preferential alignment of magnetic moment and thus spin with respect to the magnetic field. If one chirality is preferred this leads to a preferential alignment of momentum with respect to the magnetic field, and thus a current proportional to B and the chiral asymmetry.

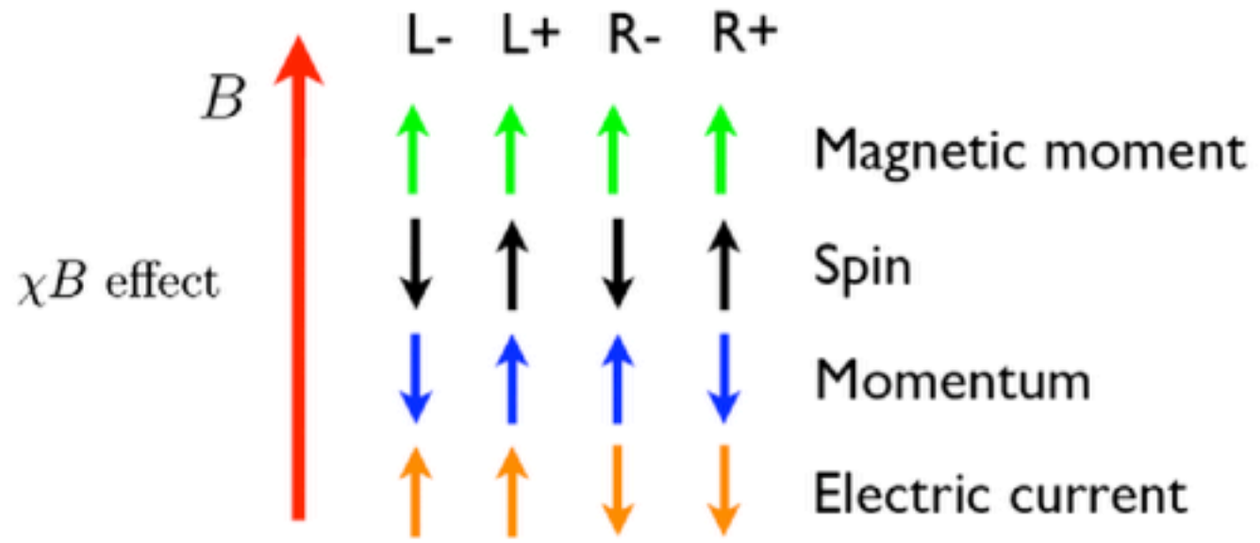

Tashiro, Vachaspati, Vilenkin, PRD 86, 105033 (2012)

FIG. 1 (color online). Understanding the χB effect. An external magnetic field tends to align the magnetic moments of the four electron states—left-right handedness for electron and positron, denoted in the figure as $L+$, $L-$, $R+$, $R-$—which implies the shown directionalities of the spin, momenta, and electric current due to each state. If the four states are present in unequal numbers, net electric current may be induced.

If in addition an electric field aligned with the magnetic field is present, momentum and thus chiral asymmetry changes which is described by anomaly equation above.

The following slides give technical details and can be skipped if only interested in the idea. They assume a cosmological context, but can easily be translated to other cases such as hot neutron stars.

For the electron chiral asymmetry $N_5 \equiv N_L - N_R$ and the magnetic helicity $\mathcal{H} \equiv \int d^3\mathbf{r}\, \mathbf{B}\cdot\mathbf{A}$ the electromagnetic chiral anomaly gives

$$\frac{d}{dt}\left(N_5 - \frac{e^2}{4\pi^2}\mathcal{H}\right) = 0\,, \tag{1}$$

and $e^2\mathcal{H}/(4\pi^2)$ is just the Chern-Simons number of the electromagnetic field. The generalized Maxwell-Ampère law

$$\boldsymbol{\nabla}\times\mathbf{B} = \frac{\partial\mathbf{E}}{\partial t} + \mu_0\left(\mathbf{j}_{\rm em} + \mathbf{j}_{cB}\right)\,, \quad \text{with} \quad \mathbf{j}_{cB} = -\frac{e^2}{2\pi^2}\mu_5\mathbf{B}\,, \tag{2}$$

and in the absence of external currents Ohm's law $\mathbf{j}_{\rm em} = \sigma\mathbf{E}$ gives

$$\mathbf{E} \simeq -\mathbf{v}\times\mathbf{B} + \eta\left(\boldsymbol{\nabla}\times\mathbf{B} + \frac{2e^2}{\pi}\mu_5\mathbf{B}\right)\,, \tag{3}$$

where $\eta = 1/(\mu_0\sigma)$ is the resistivity and the effective chemical potential is given by

$$\mu_5 = \frac{\mu_L - \mu_R}{2} - V_5 = \frac{\mu_L - V_L - \mu_R + V_R}{2}\,, \tag{4}$$

where V_5 is a possible effective potential due to a different forward scattering amplitude for left- and right-chiral electrons. Inserting this into the induction

equation the MHD is modified to

$$\partial_t \mathbf{B} = \boldsymbol{\nabla} \times (\mathbf{v} \times \mathbf{B}) + \eta \Delta \mathbf{B} - \frac{2e^2}{\pi} \eta \mu_5 \boldsymbol{\nabla} \times \mathbf{B} \,. \tag{5}$$

This equation is similar to the mean field dynamo equation which also has growing solutions. Neglecting the velocity term the evolution equations for the power spectra M_k and H_k [note $U_B = \int d \ln k M_k$ and $\mathcal{H} = \int d \ln k H_k$] now become

$$\begin{aligned} \partial_t M_k &= -\eta k^2 \left(2M_k + \frac{e^2}{2\pi^2} \mu_5 H_k \right) , \\ \partial_t H_k &= -\eta \left(2k^2 H_k + 32 e^2 \mu_5 M_k \right) . \end{aligned} \tag{6}$$

Integrating over $\ln k$ gives

$$\partial_t \mathcal{H} = -\eta \int d \ln k \left(2k^2 H_k + 32 e^2 \mu_5 M_k \right) . \tag{7}$$

In an FLRW metric these are comoving quantities and conformal time.

Now express N_5 in terms of μ_5,

$$N_5 = c(T, \mu_e) V \mu_5 \,, \quad \text{with} \quad c(T, \mu_e) = \frac{\mu_e^2}{\pi^2} + \frac{T^2}{3} \quad \text{for } \mu_e^2 + T^2 \gg m_e^2 \,, \tag{8}$$

where the second expression holds for relativistic electrons. Applying this to Eq. (1) we get

$$d\mathcal{H} = \frac{4\pi^2}{e^2} dN_5 = \frac{4\pi^2 V c(T,\mu_e)}{e^2} d\mu_5 \,. \tag{9}$$

We now take into account damping of μ_5 from *chirality flips*. In the cosmological context after electroweak breaking at $T = T_{\rm ew} \simeq 160\,{\rm GeV}$ the rate is

$$R_f \simeq \left(\frac{m_e}{6T}\right)^2 R \sim \left(\frac{m_e}{6T}\right)^2 400 \left(\frac{\alpha_{\rm em}}{6T}\right)^2 10\,T^3 \sim 10^{-4}\frac{m_e^2}{T}\,, \quad T \lesssim T_{\rm ew}\,, \tag{10}$$

which is larger than the Hubble rate. Before electroweak breaking

$$R_f \simeq \frac{T_5}{T} H(T_5)\,, \quad T \gtrsim T_{\rm ew}\,, \quad T_5 \simeq 10\,{\rm TeV}\,. \tag{11}$$

Inserting Eq. (7) into Eq. (9) then yields

$$\partial_t \mu_5 = -\frac{e^2\eta}{2\pi^2 V c(T,\mu_e)} \int d\ln k \left(k^2 H_k + 16 e^2 \mu_5 M_k\right) - 2R_f\left(\mu_5 - \mu_{5,b}\right)\,. \tag{12}$$

Here $\mu_{5,b} = -V_5 + \mu_s$ is the equilibrium value of the effective chemical potential μ_5 for $\eta \to 0$. Other processes such as electroweak interactions with other species as for example neutrinos can be taken into account by the term $\mu_{5,b}$ and thus the source term $2R_f\mu_s$.

From Eq. (6) growing solutions exist for wavenumbers

$$k < k_5 \equiv k_5(\mu_5) \equiv \frac{2e^2}{\pi}|\mu_5| \,. \tag{13}$$

This follows from using helicity modes in Eq. (5) which gives

$$\partial_t b^{\pm}_{\mathbf{k}} = \eta k \left(\mp \frac{2e^2}{\pi}\mu_5 - k \right) b^{\pm}_{\mathbf{k}} \,, \tag{14}$$

Thus if the condition Eq. (13) is fulfilled, the helicity with the opposite sign as μ_5 will grow whereas the same sign helicity will decay and the absolute value of the helicity will be close to the maximal value given by

$$|H_k| \leq \frac{8\pi M_k}{k} \,. \tag{15}$$

In contrast, for $k \gtrsim k_5$ both helicities will decay with roughly the resistive rate. For the helicity with opposite sign to μ_5 the first term in Eq. (14) corresponds to a growth rate in the cosmological context

$$R_c(k) = \frac{2e^2}{\pi}\eta k|\mu_5| \simeq 2 \times 10^{10} \left(\frac{\mathrm{TeV}}{T}\right) \left(\frac{k}{k_5}\right) \left(\frac{\mu_5}{T}\right)^2 H(T) \,, \tag{16}$$

The total rate $R_c - R_r$ reaches its maximum value $R_{\rm max} = \eta k_5^2/4$ at $k = k_5/2$ which for

$$\frac{\mu_5}{T} \gtrsim 10^{-5} \left(\frac{T}{\rm TeV}\right)^{1/2} \tag{17}$$

is larger than the Hubble rate. Furthermore, Eq. (12) shows that for growing modes $|\mu_5|$ shrinks for either sign of μ_5. Therefore, the **chiral magnetic instability transforms energy in the electron asymmetry N_5 into magnetic energy**. This is because by definition of the chemical potential μ_5 the energy U_5 associated with the chiral lepton asymmetry is given by

$$dU_5 = \mu_5 dN_5 = V c(T, \mu_e) \mu_5 d\mu_5 \,, \quad U_5 = \frac{V c(T, \mu_e) \mu_5^2}{2} \,. \tag{18}$$

Now assume that initially $\mu_5 = \mu_{5,i}$ and $U_B = 0$. Since the sign of $d\mu_5$ is opposite to the sign of $\mu_{5,i}$, Eq. (9) implies that the magnetic helicity will have the opposite sign as $\mu_{5,i}$. The growth rate peaks at wavenumber $k = k_5/2$ given by Eq. (13) and for a given mode k growth stops once $|\mu_5|$ has decreased to the point that Eq. (13) is violated. Since the instability produces maximally helical

fields saturating Eq. (15), with Eq. (9) we obtain

$$\begin{aligned} dU_B &\simeq dM_{k_5} \simeq k_5 |dH_{k_5}|/(8\pi) \simeq k_5 |d\mathcal{H}|/(8\pi) = V c(T,\mu_e)\mu_5 d\mu_5 \,, \\ \Delta E_m &\simeq \frac{V c(T,\mu_e)(\mu_{5,i}^2 - \mu_5^2)}{2} \,. \end{aligned} \tag{19}$$

Adding Eqs. (18) and (19) gives a total energy $U_{\rm tot} = U_5 + U_B \simeq V c(T,\mu_e)\mu_{5,i}^2/2$ which only depends on $\mu_{5,i}$. The maximal magnetic energy density then becomes

$$\frac{\Delta U_B}{V} \lesssim \frac{c(T,\mu_e)\mu_{5,i}^2}{2} \simeq \frac{\mu_{5,i}^2 T^2}{6} \,, \tag{20}$$

where the last expression follows from Eq. (8). Eq. (12) implies that $\partial_t \mu_5 = 0$ if

$$\tilde{\mu}_5 = \frac{R_f \mu_{5,b} - \frac{2e^2\eta}{\pi c(T,\mu_e)} \int d\ln k k \frac{M_k}{V} \left(\frac{H_k}{8\pi M_k/k} \right)}{R_f + \frac{4e^4\eta}{\pi^2 c(T,\mu_e)} \frac{U_B}{V}} \,, \tag{21}$$

where H_k has again be normalized to its maximal value given by Eq. (15). For negligible magnetic fields $\tilde{\mu}_5 \simeq \mu_{5,b}$, as expected and magnetic field modes with $k < k_5(\mu_{5,b})$ are growing exponentially with rate $R_c(k) - R_r$ given by Eq. (16). The magnetic field terms start to dominate for

$$\frac{U_B}{V} \gtrsim \frac{c(T,\mu_e) R_f}{4e^4\eta} \simeq \frac{10\pi}{3e^4} T^2 m_e^2 \simeq 2 \times 10^5 T^2 m_e^2 \,, \tag{22}$$

In this case Eq. (21) gives

$$\tilde{\mu}_5 \simeq -\frac{\pi}{2e^2 U_B} \int d\ln k k M_k \left(\frac{H_k}{8\pi M_k/k} \right) . \tag{23}$$

This is what Ruchayskiy et al call *tracking solution*. Note that $\tilde{\mu}_5$ from Eq. (21) varies with rates in general much slower than R_f and R_c. Also, since in general $\tilde{\mu}_5 \neq \mu_{5,b}$, the two terms in Eq. (12) do not vanish separately but only tend to compensate each other and are both roughly constant since μ_5 is approximately constant. Since at saturation, Eq. (23), the first term in Eq. (12) vanishes. Thus μ_5 and due to Eqs. (9) also the magnetic helicity change linearly in time with

$$\partial_t \mathcal{H} \simeq \frac{8\pi^2 V c(T, \mu_e)}{e^2} R_f (\mu_5 - \mu_{5,b}) . \tag{24}$$

Since helicity is nearly maximal this also implies that the magnetic energy also roughly grows or decreases linearly with time, depending on the sign of $(\mu_5 - \mu_{5,b})/\mathcal{H}$.

Combining Eqs. (6), (12) and (18) the rate of change of the total energy is

$$\begin{aligned}\partial_t U_{\rm tot} &= \partial_t U_B + \partial_t U_5 = \\ &= -2\eta \int d\ln k M_k \left\{ (k-k_5)^2 + 2k_5 k \left[\left(\frac{H_k}{8\pi M_k/k} \right) {\rm sign}(\mu_5) + 1 \right] \right\} \\ &\quad -2R_f V c(T,\mu_e)\mu_5 \left(\mu_5 - \mu_{5,b}\right) \,,\end{aligned} \tag{25}$$

where $k_5 = k_5(\mu_5)$ is given by Eq. (13). Since the expression in large braces is non-negative due to Eq. (15), up to the term proportional to $\mu_{5,b}$ which describes a possible energy exchange with external particles, the total energy can only decrease due to the finite resistivity and the chirality-flip rate. The only equilibrium state with $\partial_t U_{\rm tot} = 0$ is given by $\mu_5 = \mu_{5,b}$ and a magnetic energy concentrated in the mode $k = k_0 = k_5(\mu_{5,b})$ with maximal magnetic helicity with the opposite sign as $\mu_{5,b}$, $H_{k_0} = {\rm sign}(\mu_{5,b}) 8\pi M_{k_0}/k_0$.

The evolution of $\mu_{5,b}$ due to energy exchange with the background matter can be modeled as follows: In absence of magnetic fields multiplying Eq. (12) with $c(T,\mu_e)$ and using Eq. (8) gives

$$\partial_t n_5 = -2R_f [n_5 - c(T,\mu_e)\mu_{5,b}] = \pm R_w n_b - 2R_f n_5 \,, \tag{26}$$

where the gain term was written as a parity breaking electroweak rate R_w times

the number density n_b of the background lepton species. This implies

$$n_b = 2c(T,\mu_e)\frac{R_f}{R_w}|\mu_{5,b}|\,, \quad \frac{|\mu_{5,b}|}{T} \simeq 0.1 g_b \frac{R_w}{R_f}\,, \tag{27}$$

where the second expression holds for g_b non-degenerate relativistic fermionic degrees of freedom. The energy U_b associated with these background particles is thus given by

$$\frac{U_b}{V} = \int_0^{\mu_{5,b}} \mu'_{5,b} dn_b = \frac{R_f}{R_w} c(T,\mu_e)\mu_{5,b}^2 \sim 3\times 10^{-3} g_b^2 \frac{R_w}{R_f} T^4\,, \tag{28}$$

where the last expression again holds in the non-degenerate relativistic case. Note that for $\mu_{5,i} \sim \mu_{5,b} \sim (R_w/R_f)T$ Eq. (28) is of order $(R_w/R_f)T^4$ whereas U_5 from Eq. (18) is of order $(R_w/R_f)^2T^4$. Both energies vanish in the limit of parity conservation, $R_w \to 0$, as it should be. In terms of initial equilibrium chiral potential $\mu_{5,bi}$ and for $R_w \lesssim R_f$ the maximal magnetic energy is then

$$\frac{\Delta U_B}{V} \lesssim \frac{R_f}{R_w} c(T,\mu_e)\mu_{5,bi}^2 \sim 3\times 10^{-3} g_b^2 \frac{R_w}{R_f} T^4\,. \tag{29}$$

Setting $\partial_t U_b = -\partial_t U_5$ to conserve energy and equating $\partial_t U_5$ with the last term in Eq. (25) yields an equation for the evolution of $\mu_{5,b}$,

$$\partial_t \mu_{5,b} = R_w \frac{\mu_5}{\mu_{5,b}}(\mu_5 - \mu_{5,b})\,. \tag{30}$$

When U_b is included in $U_{\rm tot}$ the second term in Eq. (25) is absent in the time derivative of $U_{\rm tot}$. The total energy is then dissipated exclusively through resistive magnetic field damping. Eq. (30) indicates that $\mu_{5,b}$ typically changes with the rate R_w. A stationary state is reached if $\mu_{5,b} = \mu_5$ and the magnetic field concentrates in $k_5 = k_5(\mu_{5,b})$ with maximal helicity of sign opposite to $\mu_{5,b}$. This requires magnetic field growth rates larger than the Hubble rate, see Eq. (17).

μ_5 is continuously recreated with a rate $R_f \mu_{5,b} \sim 0.1 g_b R_w T$, see Eq. (27), and a time-independent or slowly varying μ_5 can be established which is given by Eq. (21). This can be the case, for example, in a supernova or a neutron star due to URCA processes which absorb left-chiral electrons with a rate R_w and turn them into neutrinos that subsequently escape the star.

Due to Eq. (6) amplification stops and resistive damping sets in when $2\eta k_5^2 t \sim 1$, thus

$$k_5 \sim k_5^0 \left(\frac{t_0}{t}\right)^{1/2} , \quad \mu_5 \sim \mu_5^0 \left(\frac{t_0}{t}\right)^{1/2} . \tag{31}$$

The Chiral Magnetic Effect in Hot Supernova Cores

based on Sigl and Leite, JCAP 1601 (2016) 025 [arXiv:1507.04983]

The spin flip rate is dominated by the modified URCA rate

$$\epsilon_{\rm URCA} = \frac{457\pi}{10080}(1+3g_A^2)\cos^2\theta_C G_F^2 m_n m_p \mu_e T^6\,,$$

The resistivity η=1/(4πσ) is given by the conductivity

$$\sigma \simeq 1.5\times 10^{45}\left(\frac{\rm K}{T}\right)^2\left(\frac{\rho_p}{10^{13}\,{\rm g\,cm^{-3}}}\right)^{3/2}\,{\rm s}^{-1}\,,$$

Comparing the velocity and chiral magnetic term for a velocity spectrum $v(l)\sim(l/L)^{n/2}$ for integral scale L at the length scale of maximal growth $l=2\pi/k_5=(\pi/e)^2/|\mu_5|$ gives

$$\frac{\boldsymbol{\nabla}\times(\boldsymbol{v}\times\mathbf{B})}{e^2/(2\pi^2\sigma)\mu_5\boldsymbol{\nabla}\times\mathbf{B}} \sim 2\sigma L v_{\rm rms}\left[\left(\frac{e}{\pi}\right)^2 L\mu_5\right]^{-(n/2+1)}\,,$$

For $v_{rms} \sim 10^{-2}$ in a supernova this is $\lesssim 1$ if $n \gtrsim 4/3$.

URCA to spin flip rate

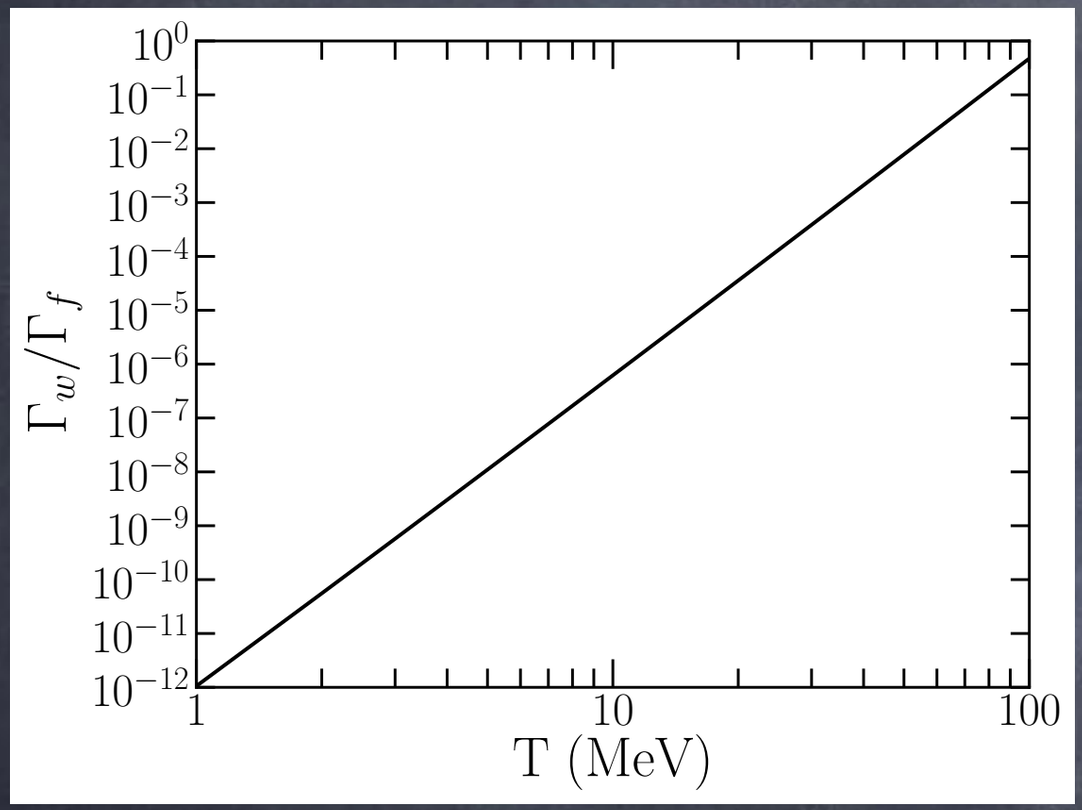

Resulting maximal field in hot neutron star within our formalism

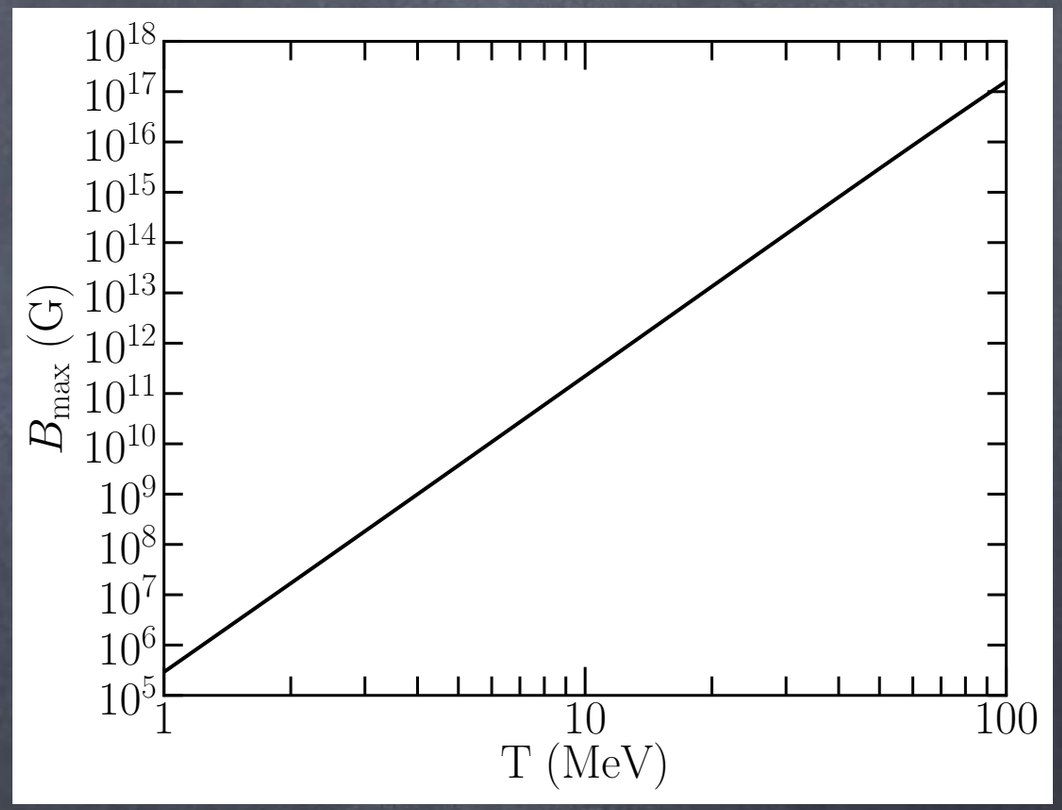

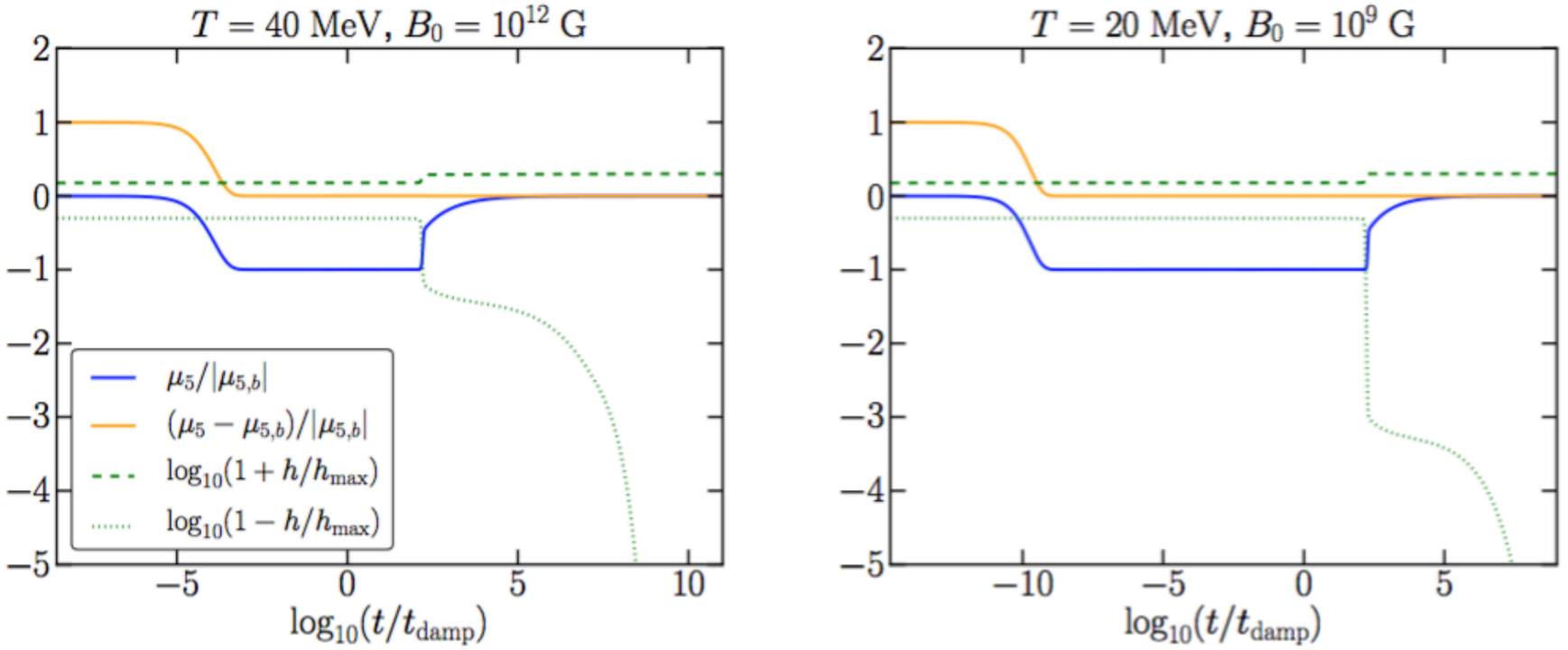

Figure 2. Time evolution of the chiral chemical potential normalized to the equilibrium value, $\mu_5/|\mu_{5,b}|$, relative difference of the chiral chemical potential to the equilibrium value, $(\mu_5 - \mu_{5,b})/|\mu_{5,b}|$ and, in logarithmic units, relative deviation of the helicity density from its maximal and minimal value, $1 \pm h/h_{\max}$. The left panel is for a temperature of $T = 40$ MeV and seed field $B_0 = 10^{12}$ G, and the right panel is for $T = 20$ MeV and a seed field of $B_0 = 10^{9}$ G.

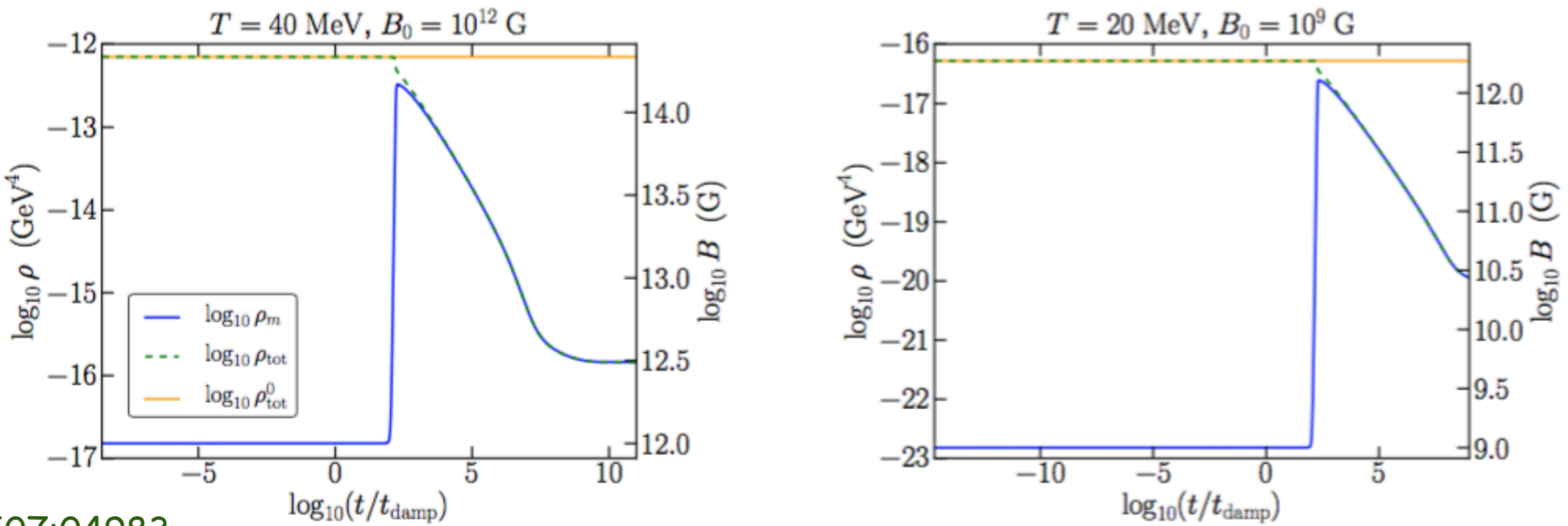

Sigl, Leite, arXiv:1507:04983

Figure 3. Time evolution of the magnetic energy density ρ_m and total energy density $\rho_{\rm tot}$. Also shown is the initial total energy density which limits the maximal magnetic energy density that can be reached by the instability. In the left panel $T = 40$ MeV and in the right panel $T = 20$ MeV.

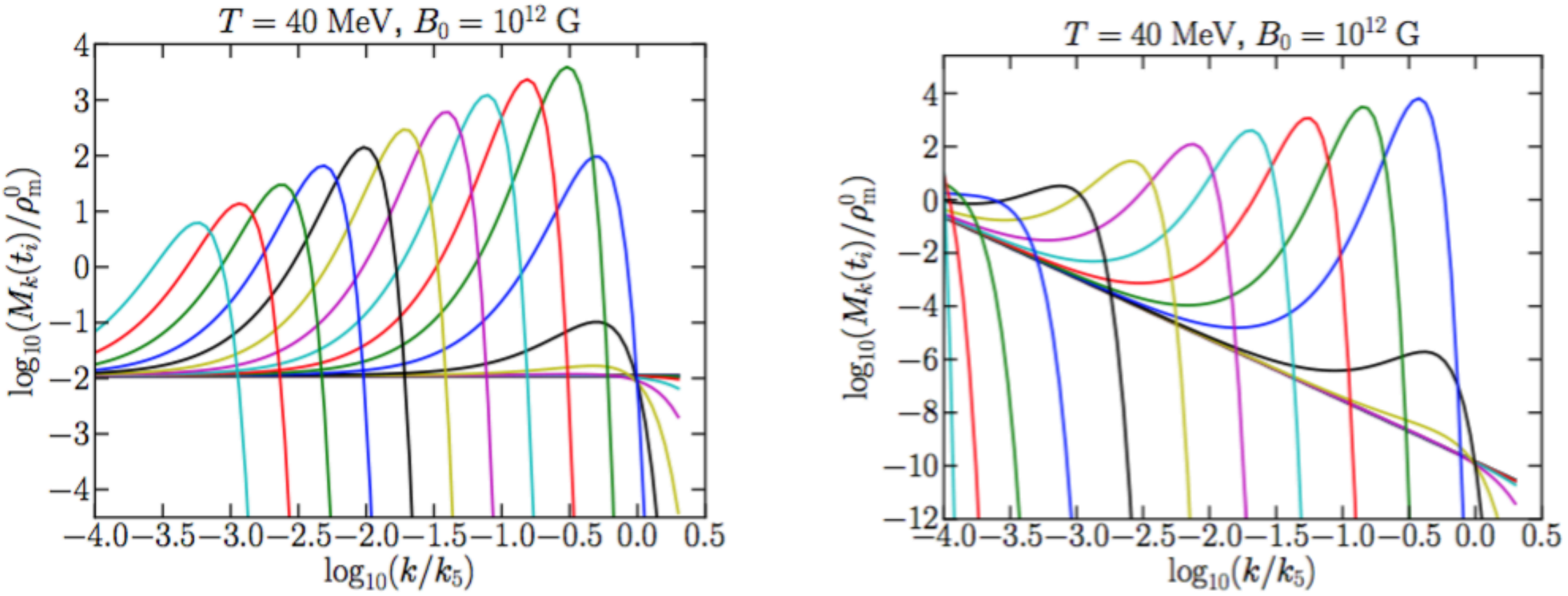

Figure 4. Time evolution of the magnetic field power spectrum normalized to the initial magnetic energy density, M_k/ρ^0_m, as a function of wavenumber k normalized to k_5. The power spectra are shown for equally spaced intervals in the logarithm of time between $t = t_{\rm damp}$ and $t = 10^8 t_{\rm damp}$, for $T = 40$ MeV. Left panel: Initially flat power spectrum. Right panel: Initial power spectrum has a Kolmogorov distribution.

The Chiral Magnetic Effect around the Electroweak Transition

We here assume that one starts with a finite μ_5 but we neglect possible contributions from a background medium, $\mu_{5,b}=0$, because contrarily to stars there is no "exterior" medium.

Conductivity $\sigma \sim 70$ T, chirality flip rates in the symmetric and broken phase; less well known in the symmetric phase

Notation for following plots:
$\Omega_m=\rho_m/\rho_{tot}=B^2/(8\pi\rho_{tot})$, $H=hV$, $h_{max}=\rho_m\, l_c = \rho_m / k_c$

based on Pavlovic, Leite, Sigl, JCAP 06 (2016) 044 [arXiv:1602.08419]

above electroweak scale (symmetric phase)

Flipping rates before the electroweak transition are determinated by inverse Higgs decays, such as $e_L\bar{e}_R \leftrightarrow \varphi^{(0)}$ and $\nu_{eL}\bar{e}_R \leftrightarrow \varphi^{(+)}$, with $\varphi^{(+)}$ and $\varphi^{(0)}$ forming the Higgs doublet. The rate of inverse Higgs decay per electron is [31, 32]

$$\Gamma_H = \frac{\pi}{192\zeta(3)} h_e^2 \left(\frac{m(T)}{T}\right)^2 , \tag{2.10}$$

where $m(T)$ is the temperature-dependent effective Higgs mass and h_e is the Yukawa coupling for electrons. There is also a contribution from scattering processes such as $t_R\bar{t}_L \leftrightarrow e_R\bar{e}_L$. This rate can be estimated from the general expression $\Gamma = n\sigma v$, where $n = \zeta(3)g_*T^3/\pi^2$ is the particle density, σ is the cross-section of the process, computed in Ref. [33] and v is the velocity of the particles involved (which at high temperatures can be taken to be of order unity), allowing us to write the rate as

$$\Gamma_{t\bar{t}} = \frac{(h_t h_e)^2 \zeta(3) g_* T^2}{8\pi^3 s} \left[\frac{s^2}{(s-m_H^2)^2 + \left(\pi h_t^2 s/16\right)^2} + 2\right] , \tag{2.11}$$

take 1-loop Standard Model electroweak results as example for 1st order phase transition

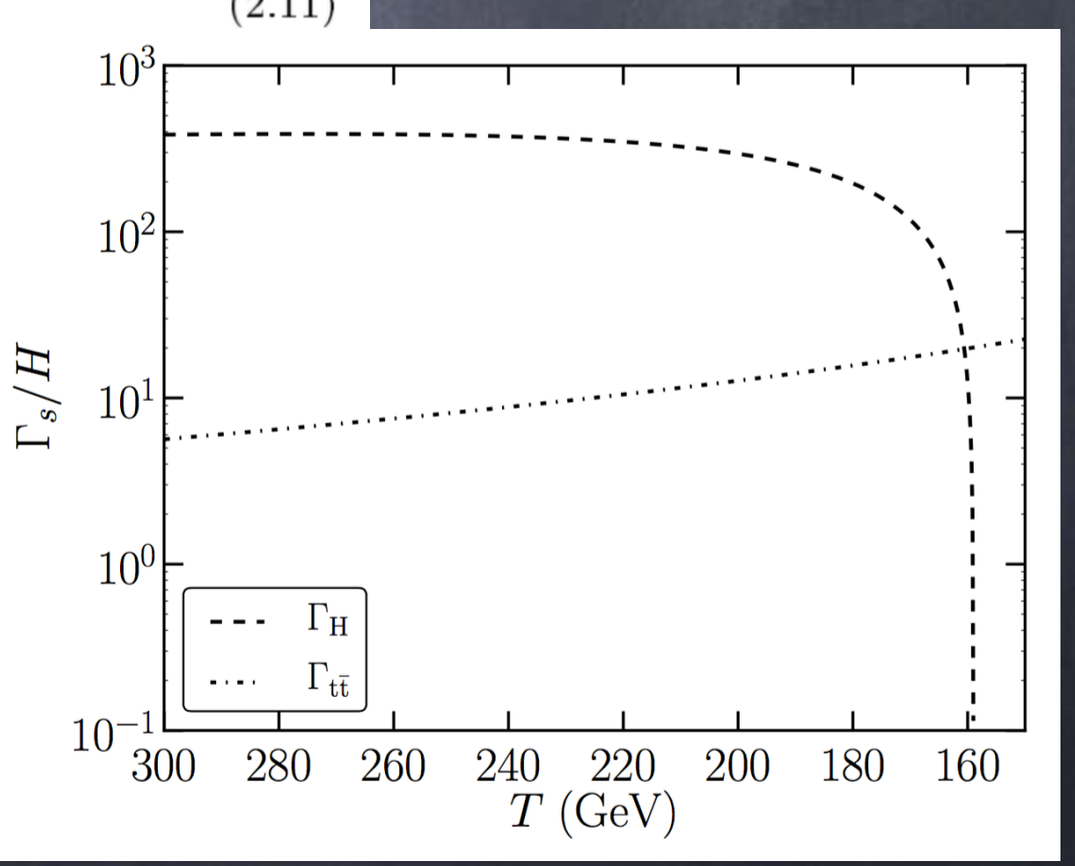

below electroweak scale (broken phase)

$$\Gamma_{\rm w} \approx G_F^2 T^4 \left(\frac{m_e}{3T}\right)^2$$

$$\Gamma_{\rm em} \approx \alpha^2 \left(\frac{m_e}{3T}\right)^2,$$

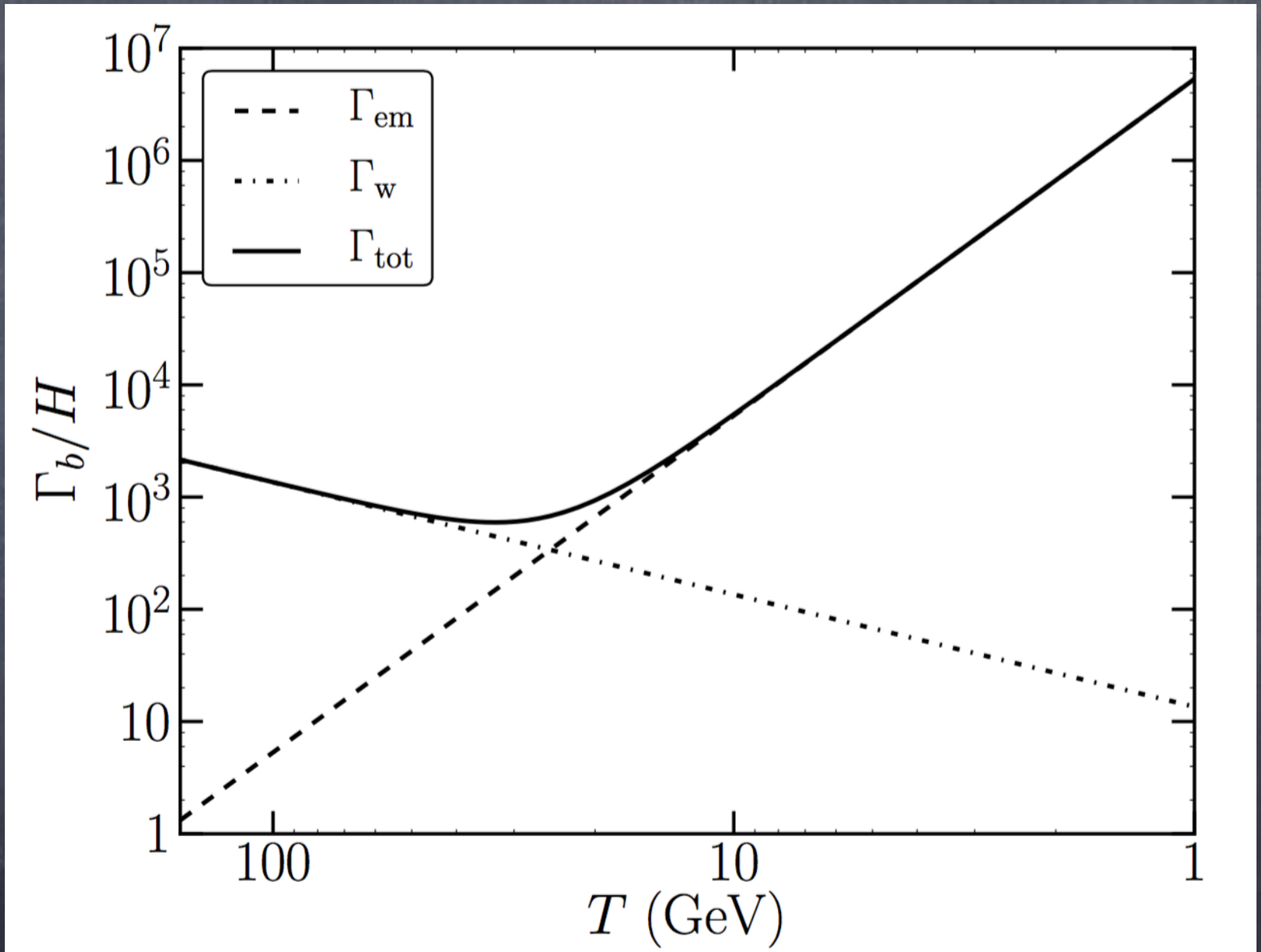

chemical potential μ_5

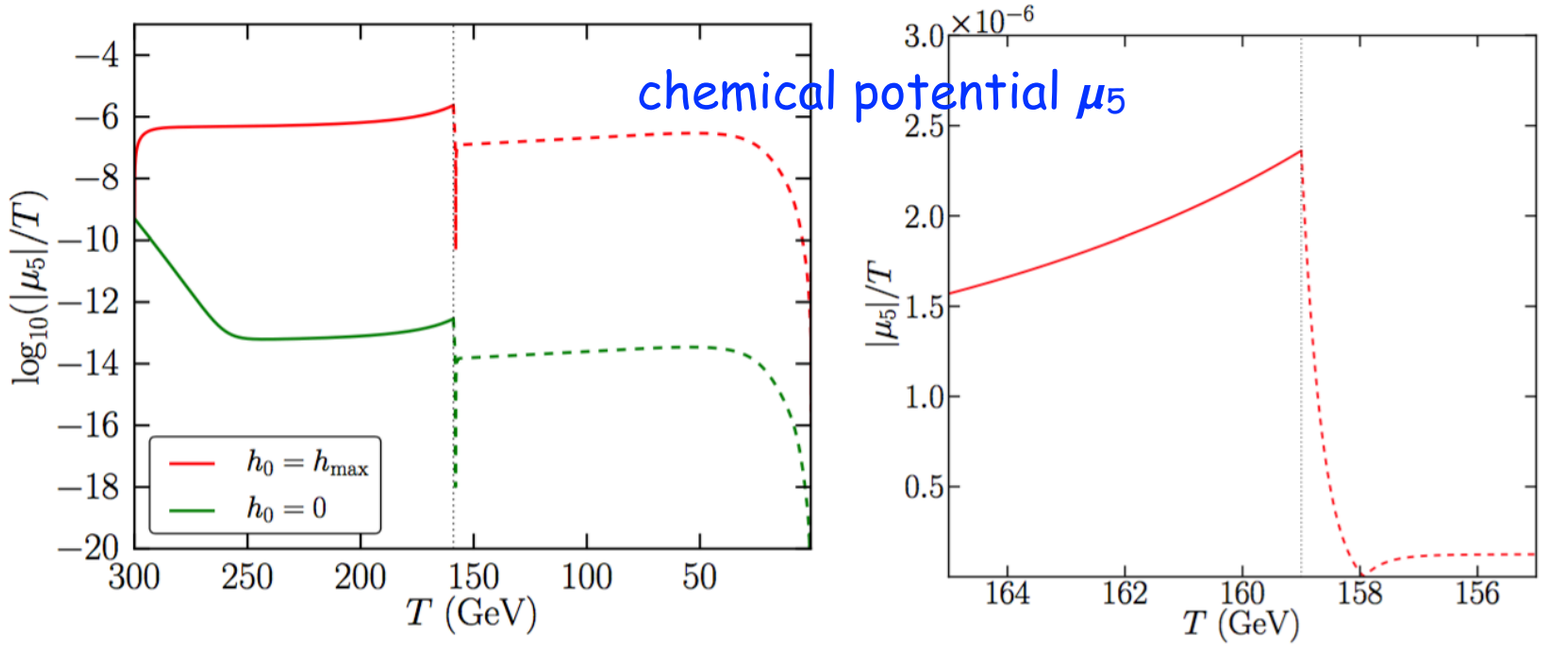

Figure 3. Evolution of the logarithm of the chiral chemical potential $\log_{10}(|\mu_5|/T)$ with temperature, before (solid lines) and after (dashed lines) the electroweak transition, with $\Omega^0_{\rm mag} = 10^{-10}$ and $\mu^0_5/T = 10^{-9}$, beginning at T =300 GeV, for the minimal initial helicity density $h^Y_0 = 0$ (in green) and maximal $h^Y_0 = h_{\max}$ (in red), on the left-hand side. Zoom around the transition for the initially maximal helical case on the right-hand side.

varying uncertain chirality flip rates for initial maximal magnetic helicity

chemical potential μ_5

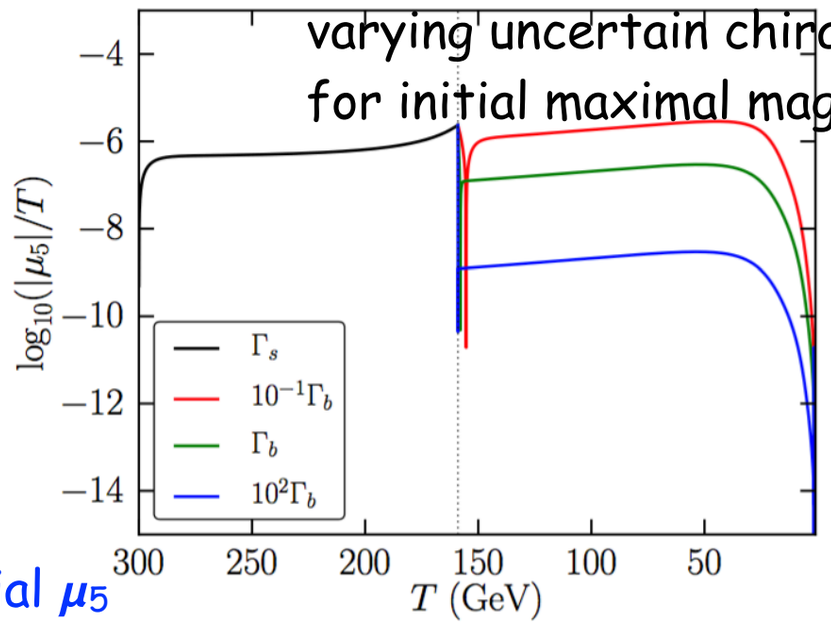

Figure 4. Evolution of the logarithm of the chiral chemical potential $\log_{10}(|\mu_5|/T)$ with temperature, with $\Omega^0_{\rm mag} = 10^{-10}$ and $\mu^0_5/T = 10^{-9}$, for the maximal initial helicity density $h^Y_0 = h_{\max}$, for different modified values of chirality flipping rates in the broken phase.

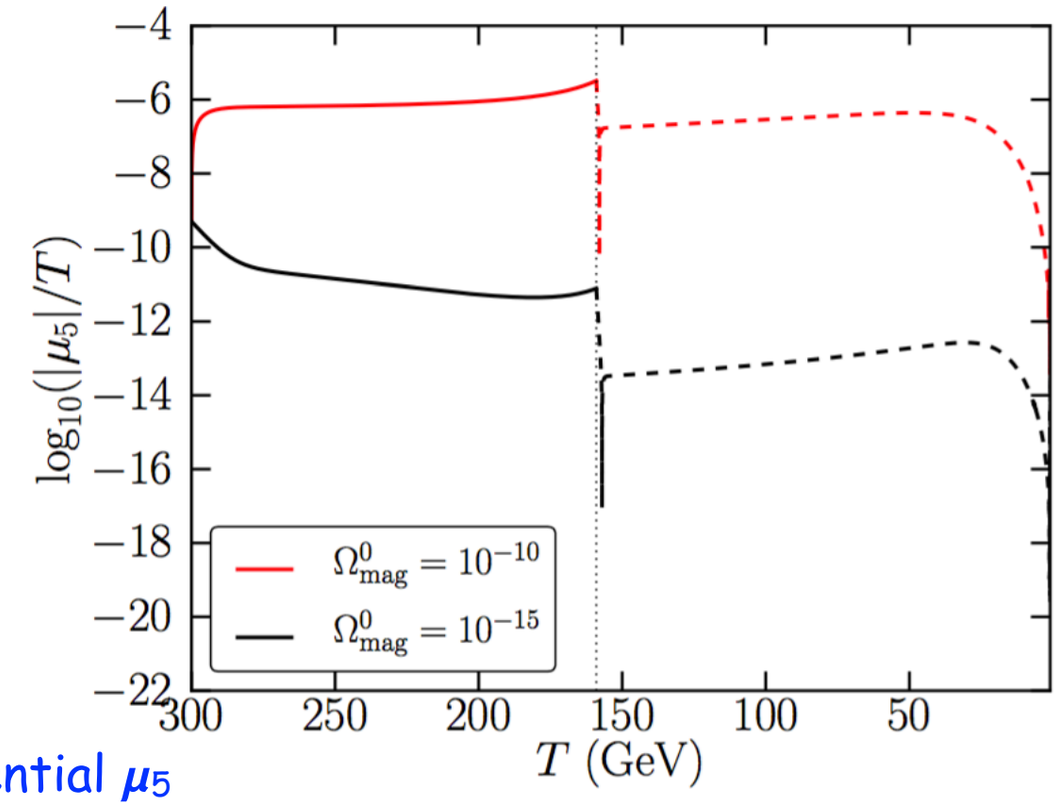

chemical potential μ_5

Figure 5. Evolution of the logarithm of the chiral chemical potential $\log_{10}(|\mu_5|/T)$ with temperature, with $\Omega^0_{\rm mag} = 10^{-10}$ in red, as in Fig. 3, and $\Omega^0_{\rm mag} = 10^{-15}$ in black, for a maximal initial helicity density and with $\mu^0_5/T = 10^{-9}$.

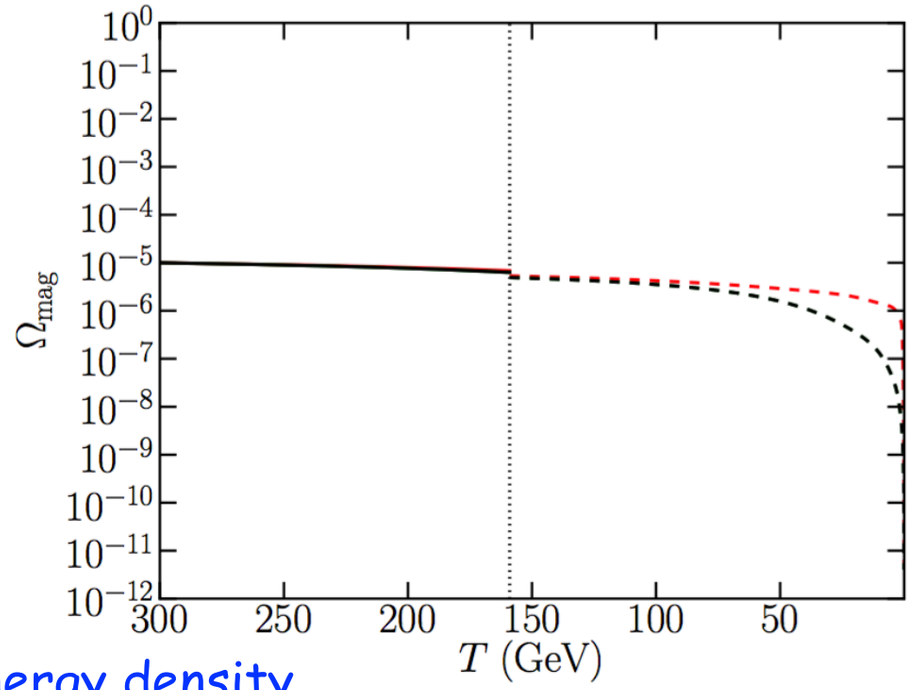

magnetic energy density

Figure 6. Evolution of the magnetic energy density normalized to the total energy density, $\Omega^{Y}_{\rm mag}$ before (solid lines) and $\Omega_{\rm mag}$ after (dashed lines) the electroweak phase transition with respect to temperature for $\Omega^{0}_{\rm mag} = 10^{-5}$ and $\mu^{0}_{5}/T = 10^{-9}$, in red. The curves in black represent the evolution of the magnetic energy density in the absence of μ_5.

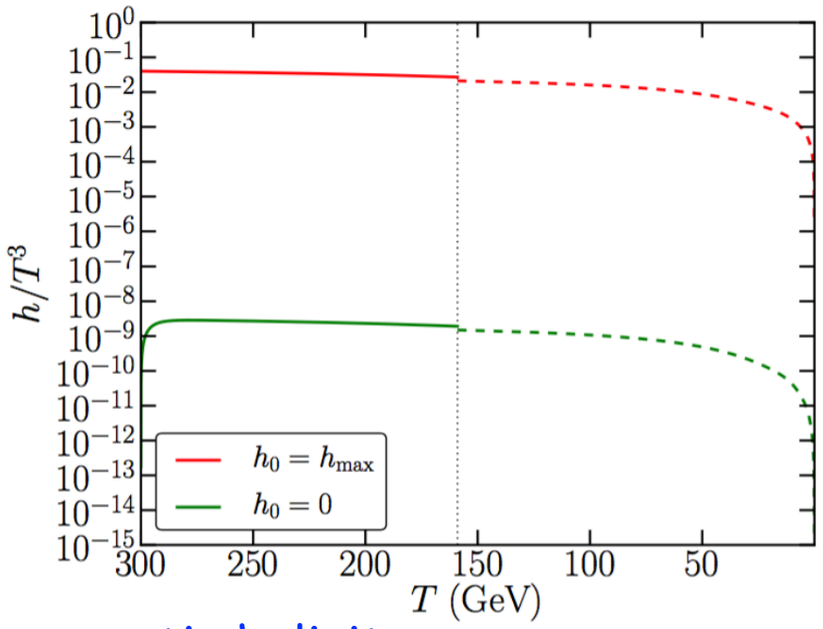

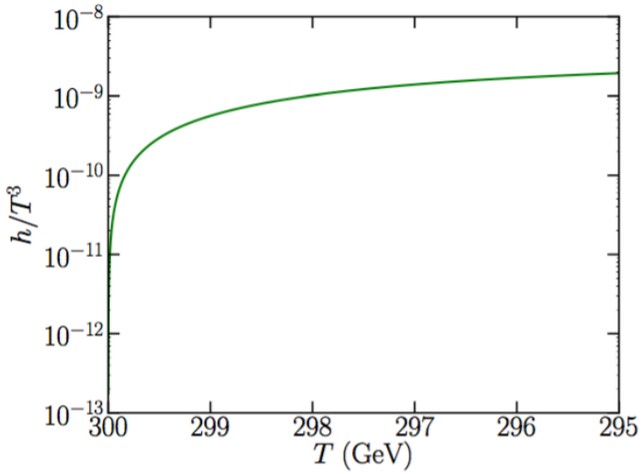

magnetic helicity

Figure 7. Evolution of helicity density, h^{Y}/T^3 before (solid lines) the electroweak transition and h/T^3 after (dashed lines) the transition for the minimal initial helicity density $h^{Y}_{0} = 0$ and maximal $h^{Y}_{0} = h_{\rm max}$, with respect to temperature and using $\Omega^{0}_{\rm mag} = 10^{-10}$ and $\mu^{0}_{5}/T = 10^{-9}$ on the left-hand side. Zoom on the high temperature region to show the helicity growth from $h^{Y}_{0} = 0$ to its later stable value on the right-hand side.

Main results for magnetic field evolution around electroweak transition:

No significant magnetic field enhancement under realistic conditions;
only resistive damping rate is somewhat slowed down;
magnetic fields tend to be helical

Open questions:

Turbulence could play a more important role than in hot neutron stars:
chiral/turbulent term > 1 only for $v_{rms} < 10^{-5}$, $\mu_5 > 0.01$ T

Role of spatially varying chiral chemical potential.

Extension to Turbulent Velocity Fields

In the drag time approximation the Lorentz force induces a velocity

$$\mathbf{v} \sim \tau_d \frac{\mathbf{j} \times \mathbf{B}}{p+\rho} = \tau_d \frac{(\boldsymbol{\nabla} \times \mathbf{B}) \times \mathbf{B}}{p+\rho} \,, \tag{32}$$

where τ_d is the response or drag time. Assuming Gaussian closure and performing the relevant Wick contractions following Campanelli this generalizes Eq. (6) to

$$\begin{aligned} \partial_t M_k &= -2\eta_{\rm eff} k^2 M_k + \frac{\alpha_+}{4\pi} k^2 H_k \,, \\ \partial_t H_k &= -2\eta_{\rm eff} k^2 H_k + 16\pi\alpha_- M_k \,, \end{aligned} \tag{33}$$

where

$$\begin{aligned} \eta_{\rm eff} &= \eta + \frac{4}{3}\tau_d \frac{U_B/V}{p+\rho} \\ \alpha_\pm &= \frac{2\eta e^2 \mu_5}{\pi} \mp \frac{1}{6}\frac{\tau_d}{p+\rho} \int d\ln k k^2 \frac{H_k}{V} \,, \end{aligned} \tag{34}$$

with V the volume of the system, see also Dvornikov and Semikoz.

Problem: this only holds for unpolarized magnetic fields, whereas in the limit of maximally helical fields Eq. (32) vanishes ! Thus Eqs. (33) are only applicable if chiral effect is sub-dominant.

Relation to Baryon and Lepton Number

There is a strong connection between gauge fields with helicity and baryon and lepton number:

$$\partial_\mu J^\mu_B(x) = \partial_\mu J^\mu_L(x) = n_f \partial_\mu K^\mu_{\rm ew} = \frac{n_f}{32\pi^2}\left(g^2 W^\alpha_{\mu\nu}\tilde{W}^{\alpha,\mu\nu} - g'^2 B_{\mu\nu}\tilde{B}^{\mu\nu}\right),$$

This violates B and L separately but conserves B-L.

Relation to Baryon and Lepton Number

based on Fujita and Kamada, Phys. Rev. D93, 083520 (2016) [arXiv:1602.02109], Phys. Rev. D94, 063501 (2016) [arXiv:1606.08891]

lepton number damping rate is dominated by electron Yukawa coupling h_e^l

$$\partial_t \eta_B \simeq -\frac{n_f \alpha_{\rm em}}{4\pi n_\gamma}\partial_t H - R_e \eta_B\,, \quad R_e \simeq |h_e^l|^2 T/(8\pi) \simeq 2\times 10^{-13} T\,.$$

In a stationary situation this gives

$$\eta_B(T) \sim \frac{16\pi n_g \alpha_{\rm em}\eta(T)}{|h_e^l|^2 n_\gamma(T) T}\left(\frac{T}{T_0}\right)^5 \left(\frac{H}{H_{\rm max}}\right)\frac{B_0^2(T)}{l_{c,0}(T)}$$

$$\sim 2.4\times 10^{-9}\left(\frac{H}{H_{\rm max}}\right)\left(\frac{B_0}{10^{-14}\,{\rm G}}\right)\left(\frac{T}{163\,{\rm GeV}}\right)^{4/3}\,,$$

where the subscript 0 refers to comoving units and T_0 is the CMB temperature today
More detailed calculations give correct baryon abundance for $B_0 \sim 10^{-17}$ G,
$l_{c,0} \sim 10^{-3}$ pc and $H \sim +H_{max}$

Conclusions 1

1.) For homogeneous and isotropic two-point correlation functions the evolution of primordial magnetic fields can be efficiently modelled within a Gaussian closure approximation.

2.) Evolution in particular of coherence scale strongly depends on helicity of magnetic fields: inverse cascades for helical fields.

3.) Helical magnetic fields may be connected to baryon and lepton numbers.

Conclusions 2

1.) The chiral magnetic effect can lead to growing, helical magnetic fields in the presence of a chiral asymmetry in the lepton sector.

2.) However, spin flip interactions can damp the chiral asymmetry faster than the magnetic field growth rate.

3.) In hot supernova cores the chiral magnetic effect could play a significant role. This is less likely in the early Universe.

4.) Still, for $\mu_5/T > 10^{-9}$ one could obtain almost maximally helical field and for $B_0 \sim 10^{-16}$ G one obtains right order of magnitude baryon number.

Outlook/Open Questions

1.) Role of turbulence unclear: If velocity term > chiral term the chiral magnetic effect could be considerably modified. Suppression if magnetic fields transported toward smaller scale ? Enhancement if transported toward larger scales (inverse cascade) ?

2.) Role of fermion mass: strictly speaking in thermodynamic equilibrium one can define μ_5 only if m=0 identically which is not the case. Is there a discontinuous change of physics at m=0 ?

3.) Spatially varying chiral potential should be discussed quantitatively